

On the diversity of short GRBs

Stephan Rosswog¹ and Enrico Ramirez-Ruiz²

¹*Department of Physics and Astronomy, University of Leicester, LE1 7RH, Leicester, UK.*

²*Institute of Astronomy, Madingley Road, Cambridge, CB3 0HA, UK.*

ABSTRACT

Hydrodynamical simulations of the last inspiral stages and the final coalescence of a double neutron star system are used to investigate the power of the neutrino-driven wind, the energy and momentum of the fireball produced via $\nu\bar{\nu}$ -annihilation, and the intensity and character of their interaction. It is argued that the outflow that derives from the debris will have enough pressure to collimate the relativistic fireball that it surrounds. The low luminosity relativistic jet will then appear brighter to an observer within the beam although most of the energy of the event is in the unseen, less collimated and slower wind. This model leads to a simple physical interpretation of the isotropic luminosities implied for short GRBs at cosmological distances. A wide variety of burst phenomenology could be attributable to the dependence of the neutrino luminosity on the initial mass of the double NS binary.

Key words: dense matter; hydrodynamics; neutrinos; gamma rays: bursts; stars: neutron; methods: numerical

1 INTRODUCTION

Gamma-ray bursts (GRBs) come in two basic types with short (≤ 2 s) and long (≥ 2 s) duration (Kouveliotou et al. 1993). So far, only the latter class has been relatively well-studied – several *long* bursts have been associated with afterglows that have been observed from radio frequencies to X-ray energies (see Mészáros 2002 for a recent review). By contrast recent X-ray, optical and radio searches have not yet been successful for short GRBs (although see Lazzati, Ramirez-Ruiz & Ghisellini 2001). These bursts – which make up about one-third of all observed GRBs – differ markedly from the long ones not only in duration but also in having a larger fraction of high-energy gamma rays in their energy distribution. The most widely discussed possibility is that they result either from the merger of two compact neutron stars or of a neutron star (NS) and a black hole (BH; Lattimer & Schramm 1976; Paczyński 1986, 1991; Eichler et al. 1989; Narayan, Paczyński & Piran 1992; Mochkovitch et al. 1993; Kluźniak & Lee 1998; Rosswog et al. 1999; Ruffert & Janka 1999; Lee & Ramirez-Ruiz 2002; Rosswog & Davies 2002).

The merger of two neutron stars produces a remnant with huge energy reservoirs. The difficult question to answer is how gravity and spin can conspire to form the outflowing relativistic plasma that is required to explain the observations. The conventional view is that the released energy is quickly and continuously transformed into a radiation-dominated fluid with a high entropy per baryon (Cavalo & Rees 1978). This *fireball* is then collimated into a pair of anti-parallel jets. There is as yet no universally accepted explanation for jet collimation. The difficulty of the problem is that there are interactions between the central object (black hole or other), the inflow (i.e. disk), the outflow (i.e. wind) and the jet, and most of the dissension comes about assessing condition and strength of these interrelationships (e.g. Blandford 2002). Particular importance is attached here to the interaction of the jet with the less collimated and slower outflow associated with the disk. The most prominent feature of such interaction is that the wind may be responsible for collimating the jet (Levinson & Eichler 2000; hereafter LE), and it is to this problem that we have turned our attention.

We used three-dimensional high-resolution calculations of NS coalescences to study the neutrino emission from the hot merger remnant of a NS binary encounter. The issues we investigate here include the properties of the neutrino-driven outflow (from the debris), the energy and momentum injected into the region above the remnant via $\nu\bar{\nu}$ annihilation, and the intensity and character of their interaction. We estimate the dependence of the neutrino luminosity on the initial mass of the double NS binary and discuss the possible variety of afterglow behaviour that is expected from fireballs that are collimated by a surrounding baryonic wind. Our findings may be useful for designing search strategies for detecting the afterglows of short GRBs.

2 NEUTRINO EMISSION IN NS COALESCENCE

We have recently performed a series of three dimensional, high-resolution simulations of the last inspiral stages and final coalescence of a double NS using the smoothed particle hydrodynamics method with up to $\approx 10^6$ particles (the reader is referred to Rosswog & Davies 2002 for further details on the hydrodynamic evolution). Aware of its decisive role in the thermo-dynamical evolution of the debris, we have used a *realistic* equation of state for hot, dense nuclear matter, which is based on the tables provided by (Shen et al. 1998a,b) and smoothly extended to the low density regime with a gas consisting of neutrons, alpha particles, photons and e^\pm pairs.

Under the conditions encountered in the merger neutrinos are emitted copiously and provide the most efficient cooling mechanism for the dense, shock- and shear-heated debris. Moreover, the related weak interactions determine the compositional evolution which is altered by reactions such as electron and positron captures. The effect on the cooling and the changes in the composition of the material are taken into account via a detailed multi-flavour neutrino treatment which is described in detail in Rosswog & Liebendörfer (2003). The results presented here are based on the close analysis of late time segments, typically a time $t_{\text{sim}} \approx 15$ ms after the start of the merger simulations. Results are described from three representative runs: first, an initially corotating system with twice $1.4 M_\odot$ (c1.4), second, a system with twice $1.4 M_\odot$ and no initial NS spins (i1.4), which we regard as the generic case and finally, as an extreme case, a system of twice $2.0 M_\odot$ and no initial spins (i2.0). In addition, in §4 a set of less resolved simulations is used to explore the dependence of the neutrino luminosity on the system mass.

The debris is heated initially via shocks (for example when two spiral arms merge supersonically, see Fig. 13 in Rosswog & Davies 2002) and later via shear motion. The innermost part of the debris torus is heated via shocks (to $T \approx 3$ MeV) that emerge when cool, equatorially inflowing material collides with matter being shed from the central object. The cool equatorial inflow ($T < 1$ MeV) allows for the presence of heavy nuclei with a mass fraction of $\approx 10\%$ and mass numbers of $A \approx 80$ and $Z/A \approx 0.3$. Most parts of the inner disk are essentially dissociated into neutrons and protons. We find neutrino luminosities of $\approx 10^{53}$ erg s $^{-1}$ which are dominated by electron anti-neutrinos (Rosswog & Liebendörfer 2003). The mean energies are around 8, 15, and 22 MeV for electron neutrinos, electron anti-neutrinos and the heavy lepton neutrinos, respectively. Figure 1 shows the total neutrino energy per time and volume in the orbital and meridional planes of the merged remnant of our generic case (i1.4). The neutrino emission provides the driving stresses that will lead to both a relativistic outflow (through $\nu\bar{\nu}$ -annihilation) and a less collimated (and slower) outflow associated with the debris.

2.1 $\nu\bar{\nu} \rightarrow e^+e^-$ above the remnant

The neutrino annihilation process (which scales roughly with L_ν^2) can tap the thermal energy of the hot debris. The presence of a region of very low density along the rotation axis, away from the equatorial plane of the debris must be present when the burst takes place or otherwise prohibitive baryon loading will happen. The centrifugally evacuated funnel region above the remnant is an attractive place for this deposition to occur because it is close to the central energy source (the energy deposition rate scales roughly with the inverse fourth power of the distance) but contains only a small number of baryons (e.g. Davies et al. 1994, Ruffert et al. 1997, Rosswog and Davies 2002).

The ratio of e^\pm energy deposition to baryon rest mass energy, $\eta = Q_{\nu\bar{\nu}}\tau_{\text{inj}}/(\rho c^2)$, in the region above the poles of the merged remnant is shown in Figure 1. ρ denotes the matter density and, for simplicity, an energy injection time, $\tau_{\text{inj}} = 1$ s has been assumed (Rosswog & Ramirez-Ruiz 2002). The copiously emitted electron neutrinos and anti-neutrinos dominate the annihilation process by $\approx 95\%$, their mean average energies $\langle E \rangle$ being ≈ 8 MeV for ν_e and ≈ 15 MeV for $\bar{\nu}_e$.

Due to the finite resolution of the simulations the densities along the rotation axis are overestimated since they are mainly determined by particles located in the inner parts of the disk. The above restriction causes η to be undervalued. Typical luminosities of $\approx 10^{47}$ erg s $^{-1}$ (c1.4), $\approx 3 \times 10^{48}$ erg s $^{-1}$ (i1.4), $\approx 10^{49}$ erg s $^{-1}$ (i2.0) are found in the fireball region with $\eta > 1$. The largest attainable Lorentz factors (≈ 15 although larger values are expected from higher numerical resolution) are found along the binary rotation axis yet at large angles away from it an increasing degree of entrainment leads to a drastic decrease in η (Fig. 1). The jet is likely to develop a velocity profile so that different parts move with different Lorentz factors. During the early stages of its evolution, this entrainment is expected to give rise to a mixing instability which could provide erratic changes in the relativistic jet velocity that would manifest in internal shocks.

2.2 Neutrino-driven wind

The neutrinos that are emitted from the inner regions of the torus will deposit part of their energy in the outer parts of the thick disk that has formed around the central object. For example, a nucleon located at ≈ 100 km from the central object gains the equivalent of its gravitational binding energy by capturing 3 neutrinos of ≈ 15 MeV. Similar to the neutrino heating mechanism in core-collapse supernovae, such neutrino deposition will drive a strong mass outflow. For high luminosities ($L_\nu > 10^{52}$ erg s $^{-1}$), the mechanical power of the neutrino-driven wind $L_w = 1/2\dot{M}v_w^2$ (where v_w is the asymptotic velocity) is found to be largely independent of mass (Thompson et al. 2001) with $L_w \propto L_\nu^\alpha$ and $\frac{16}{5} < \alpha < \frac{17}{5}$. Using Thompson et al. (2001) Table 1 we find $L_w = 2.0 \times 10^{49}$ erg s $^{-1} L_{\nu,53}^{16/5}$. This yields a wind mechanical power of $\approx 2 \times 10^{49}$ erg s $^{-1}$, $\approx 2 \times 10^{50}$ erg s $^{-1}$, and $\approx 2 \times 10^{51}$ erg s $^{-1}$ for runs c1.4, i1.4 and i2.0.

While the above estimates agree with other estimates derived in the context of proto-neutron star formation (e.g. Duncan, Shapiro & Wassermann 1986; Qian & Woosley 1996) they do not take into account the specific geometry of a merger remnant nor the extreme neutron

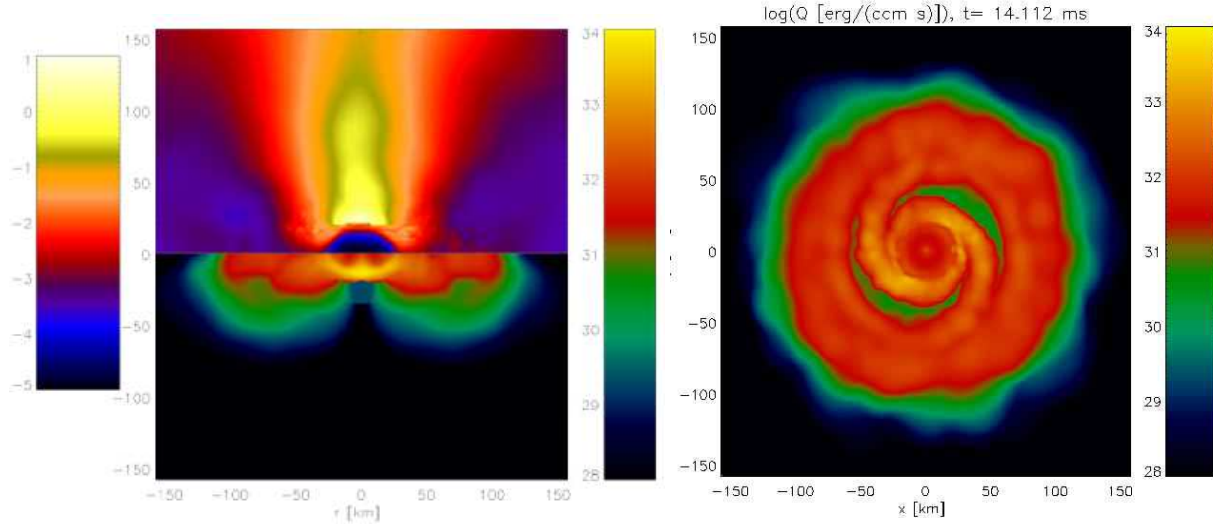


Figure 1. Geometry of the neutrino emission above the merged remnant of model i1.4 (2x 1.4 M_\odot , no spin). The right panel shows the logarithm of the total neutrino energy emitted per time per volume (cgs units) from the orbital plane while the left panel displays the meridional plane. The upper half-plane of the left panel shows the ratio of energy deposited during τ_{inj} via $\nu\bar{\nu} \rightarrow e^+e^-$ to rest mass energy, η , which is a measure of the maximum attainable Lorentz factor. The colourbar on the left of this panel refers to $\log(\eta)$. The lower half-plane of the left panel shows the total neutrino emission in meridional plane. The colour coding is the same as in the right panel.

richness of the debris, we expect the corresponding correction factors to be of order unity, which we consider accurate enough for the following discussion.

3 THE JET-WIND CONNECTION

We have now all the ingredients to consider the interaction of the jet with the less collimated and slower outflow associated with the debris. The most prominent feature of this interaction is that the wind may be responsible for collimating the jet (LE). The collision of the two fluids will lead to the formation of a contact discontinuity across which the total pressure is continuous. Besides, two oblique shocks, one in each fluid, will form across where the streamlines of the colliding (unshocked) fluids are deflected. The structure of the shocked layers will depend on the parameters of the two outflows and on the boundary conditions.

On the condition that the baryonic wind is highly supersonic not too far out the streamlines of the colliding fluids, the momentum transfer by the wind into the jet is dominated by ram pressure. The ram pressure of the baryonic outflow just upstream the oblique shock at the axial coordinate z is then given by (LE)

$$(p_w + \rho_w c^2) U_w^2 = \beta_w L_w / (4\pi^2 c a_c r), \quad (1)$$

where p_w , $\rho_w c^2$, and U_w the corresponding wind pressure, energy and four-velocity, r is the distance between the torus and the nearest point at the shock, $a_c(z)$ is the cross-sectional radius of the contact discontinuity surface, and β_w is the wind terminal velocity (which is set to the escape velocity of the system in the following estimates).

If the shocked wind layer is very thin due to rapid cooling of the gas and using the requirement that the total pressure must be continuous across the contact discontinuity, LE balance entropy and energy fluxes to obtain: $\theta \approx \pi \beta_w^{-1} (L_j / L_w)$, where θ is the jet opening angle at large distances and the Lorentz factor at the base of the jet has been assumed to be of order unity (this approximation is justified in Rosswog & Ramirez-Ruiz 2002).

In the above estimate L_w is the total wind power emanating from a thin torus of radius R centred around the central object. This geometry is reminiscent of the neutrino emission structure seen in Figure 1. Neutrinos emitted from the most luminous ring-like region at about $R \approx 25$ km drive a baryonic outflow whose total wind power surpass that ejected from rest of the debris by at least an order of magnitude. Numerical integration of equation (1), where the neutrino-driven wind is assumed to arise from a sequence of concentric rings located at $z = 0$, confirms that the ring with the highest wind power determines the properties of the cross-sectional radius of the jet at large distances ($z > R$). To first order we therefore estimate L_w to be the total wind power emanating from this thin and most luminous region. In this way, at large enough distances from the plane of the remnant, the semi-aperture angle of the wind-confined jet is given by

$$\theta \approx 0.3 \beta_{w,-1}^{-1} L_{w,50}^{-1} L_{j,48.5}, \quad (2)$$

where we adopt the convention $Q = 10^x Q_x$, using cgs units. Once the fireball Lorentz factor exceeds θ^{-1} , it will remain conical with the

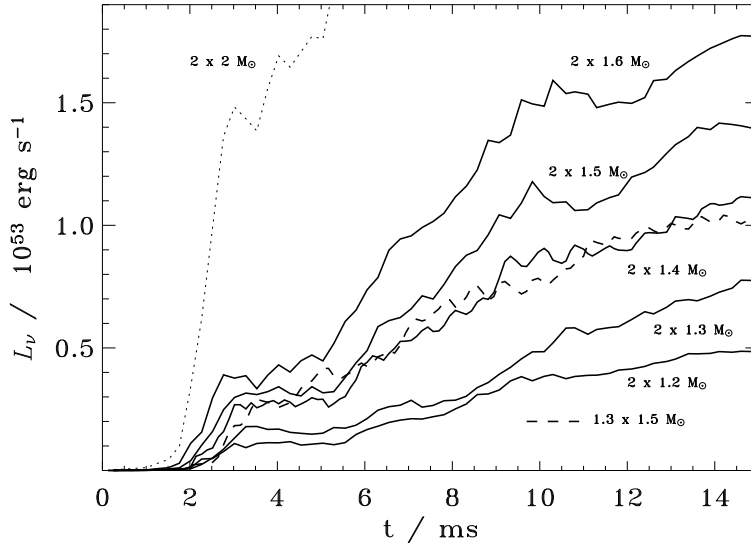


Figure 2. Total neutrino luminosities as functions of time for various NS/NS merger masses. The merger calculations were performed using a SPH method with $\sim 6 \times 10^4$ particles.

same opening angle regardless of the external conditions. This occurs at a distance $\sim R\theta^{-1}$ from the engine, which in turn implies that the baryonic outflow needs to develop $t \sim 3R_1\beta_{-1}^{-1}\theta_{-1}^{-1}$ ms before the explosion that forms the GRB. This requirement is justified by the fact that the neutrino luminosities reached their maximum, stationary level $t > 15$ ms after the start of the simulations (see Fig. 2).

It is therefore likely that the neutrino-driven outflow that develops in the merged debris will have enough pressure or inertia to provide collimation. The beaming fraction is given by $\varsigma = \Omega/2\pi \approx (\pi^2/2)(L_j/\beta_w L_w)^2$ and hence the apparent luminosity is $L_\Omega \approx L_j \varsigma^{-1} = 2 \times 10^{49} \beta_{w,-1}^2 L_{w,50}^2 L_{j,48}^{-1} \text{ erg s}^{-1}$. The above estimate gives $\theta \approx 0.1$ (≈ 0.02) and $L_\Omega \approx 10^{51} \text{ erg s}^{-1}$ ($L_\Omega \approx 3 \times 10^{52} \text{ erg s}^{-1}$) for runs i1.4 and i2.0 (assuming $\alpha = 16/5$), which clearly satisfies the apparent isotropized energies of $\approx 10^{51}$ erg implied for short bursts at $z = 1$ (Panaitescu et al. 2001; Lazzati et al. 2001).

The above reasoning does not take into account effects associated with the formation of a rarefaction wave in the baryonic wind near the interface separating the two fluids. This will depend on the properties of the solution near the object and could result in a steeper decline of the pressure supporting the jet, and the consequent alteration of the profile at the contact discontinuity. There will also surely be some entrainment of the electron-ion fireball plasma and this should ultimately show up in the polarization observations which can, in principle distinguish a pair plasma from a protonic plasma. Entrainment will be promoted by linear instabilities that could grow at the jet surface (Appl & Camenzind 1993). In addition, there can be an exchange of linear momentum with the surrounding outflow, even if there is minimal exchange of mass. This can develop a velocity profile in the jet so that different parts move with different Lorentz factors.

4 DIVERSITY OF AFTERGLOW BEHAVIOUR

The framework we have used to determine the geometry and energetics of short GRBs is a simple one. Given the limitations of our assumptions we draw three conclusions. First, an inner relativistic jet collimated by a surrounding baryonic wind can appear brighter to the observer by a factor that is inversely proportional to its intrinsic power (LE). Second, a modestly broad distribution of neutrino luminosities can result in a wide variety of opening angles and apparent luminosities. This can be understood as follows: the luminosity of the $\nu\bar{\nu}$ -annihilation jet increases as L_ν^2 while $L_w \propto L_\nu^\alpha$, so that $\theta \propto L_\nu^{\alpha-2}$ and $L_\Omega \propto L_\nu^{2\alpha-2}$ ($\frac{16}{5} < \alpha < \frac{17}{5}$). Third, only a small fraction of bursts are visible to a given observer with most of the energy of the event being in the unseen outer outflow.

Figure 2 shows the results of a set of test calculations (with $\sim 6 \times 10^4$ particles, no initial spin) performed in order to explore the effect that the masses of the neutron stars in the merging binary have on the total neutrino luminosity. From these models we derived an approximate relation between L_ν and the total mass of the compact binary, which we then apply to estimate the possible variety of afterglow behaviour that could be expected from NS-NS mergers.

We set up a 10^6 grid of initial binary masses chosen according to the theoretical distribution function of NS derived by Fryer & Kalogera (2001). The compact-remnant distribution is dominated by NSs in the mass range $1.2-1.6 M_\odot$ and falls off drastically at higher

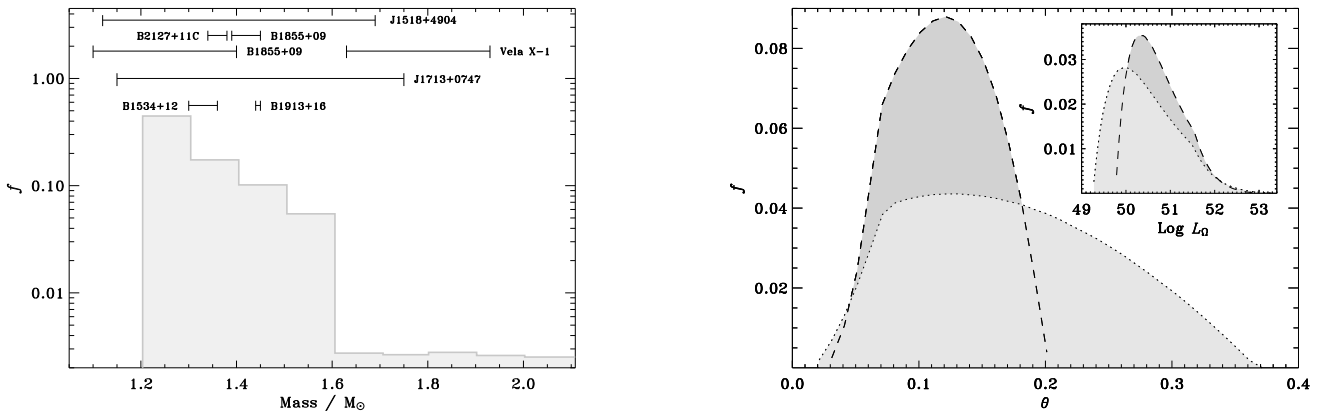


Figure 3. Isotropic luminosities implied for short GRBs understood in terms of collimation of the fireball by an outer baryonic outflow. The left panel shows the distribution of neutron-star remnant masses derived by Fryer & Kalogera (2001). The NS masses are measured by Thorsett & Chakrabarty (1999) and Barziv et al. (2001). The right panel shows the distribution of expected opening angles and luminosities for NS binaries. The dashed line assumes $L_w \propto L_\nu^{16/5}$ while the dotted line uses $L_w \propto L_\nu^{17/5}$.

remnant masses (Fig. 3). Under the assumption that the total neutrino luminosity (at late times) depends primarily on the total mass of the compact binary (note that this is a reasonable assumption for mergers of unequal masses provided that the binary mass ratio is not extreme; see Fig. 2) and that $L_w \propto L_\nu^\alpha$ (Thompson et al. 2001), we derive the distribution of opening angles and luminosities expected from such encounters. Our results for two values of α (16/5 and 17/5) are shown in Figure 3.

Since the jets are visible to only a fraction ς of the observers, the true GRB rate $R_\tau = \langle \varsigma \rangle^{-1} R_{\text{obs}}$, where R_{obs} is the observed rate and $\langle \varsigma \rangle^{-1}$ is the harmonic mean of the beaming fractions. We find $\langle \varsigma \rangle^{-1} \sim 100$. Following Schmidt (2001) $R_{\text{obs}}(z=0) = 0.5 \text{ Gpc}^{-3} \text{ yr}^{-1}$. The true rate is then $R_\tau(z=0) \sim 50 \text{ Gpc}^{-3} \text{ yr}^{-1}$, which should be compared with the estimated rate of NS coalescence $R_{\text{NS}}(z=0) \sim 80 \text{ Gpc}^{-3} \text{ yr}^{-1}$ ($\sim 2 \times 10^{-5} \text{ yr}^{-1}$ per galaxy; Phinney 1991). We note that the simple collimation mechanism presented here provides an adequate description of the observations.

5 SUMMARY

In this letter we consider the viability of NS-NS binary coalescences as central engines of short GRBs. The main form of energy release we regard is neutrino emission from the disk¹.

We suggest that the isotropic luminosities implied for short GRBs at cosmological distances can be understood in terms of collimation of the $\nu\bar{\nu}$ -annihilation fireball by the neutrino-driven wind. We argue that the existence of such a baryonic wind is a natural consequence of the huge gravitational binding energy released in the form of neutrinos.

Moreover, we show that the wind derived from the disk could in principle have enough pressure or inertia to provide collimation to the fireball that derives from the region around the BH. In other words, bursts produced by such a mechanism are not isotropic but instead beamed within a solid angle, typically ~ 0.1 sterad. Within the framework of this simple model we have deduced the distribution of opening angles and luminosities expected from $\nu\bar{\nu}$ -annihilation in NS-NS mergers and uncovered that within the uncertainties of the calculations, the coalescence scenario is capable of providing the required isotropized energies and a compatible number of progenitors.

Given the few hundred kilometres per second acquired by the NS at birth and assuming a typical coalescence time of about 100 Myr, these bursts should occur predominantly in the low-density halo of the galaxy. The external shock can therefore occur at much larger radii and over a much longer timescale than in usual afterglows, and the X-ray intensity is below the threshold for triggering. Alternatively, the burst could go off inside a pulsar cavity inflated by one of the neutron stars in the precursor binary. Such cavities can be as large as fractions of a parsec or more, giving rise to a deceleration shock months after the GRB with a consequently much lower brightness that could avoid triggering and detection. In conclusion, the absence of detected afterglows in short bursts is not surprising, and, as argued above, a wide diversity of behaviours may be the rule, rather than the exception.

¹ More energy could be pumped into the $e^\pm\gamma$ fireball when the rapidly rotating BH is formed or if magnetic field are able to tap the rotational energy of the BH with higher efficiency than $\nu\bar{\nu}$ does (Popham, Woosley & Fryer 1999; Rosswog, Ramirez-Ruiz & Davies 2003).

ACKNOWLEDGEMENTS

It is a pleasure to thank M. J. Rees & A. MacFadyen for discussions and the Leicester supercomputer team S. Poulton, C. Rudge and R. West for their excellent support. The computations reported here were performed using both the UK Astrophysical Fluids Facility (UKAFF) and the University of Leicester Mathematical Modelling Centre's supercomputer. This work was supported by PPARC, CONACyT, SEP and the ORS foundation.

REFERENCES

Appl S., Camenzind M., 1993, *A&A*, 274, 699
 Barziv O., Kaper L., Van Kerkwijk M. H., Telting J. H., Van Paradijs J., 2001, *A&A*, 925
 Blandford R. D., 2002, in Chang-Hwan L., Heon-Young C., eds, *Current high-energy emission around black holes*, World Scientific, p. 199
 Cavallo G., Rees M. J., 1978, *MNRAS*, 183, 359
 Duncan R. C., Shapiro S. L., Wassermann I., 1986, *ApJ*, 309, 141
 Eichler D., Livio M., Piran T., Schramm D. N., 1989, *Nature*, 340, 126
 Fryer C. L., Kalogera V., 2001, *ApJ*, 554, 548
 Klužniak, W. & Lee, W. H. 1998, *ApJ*, 494, L53
 Kouveliotou, C., et al., 1993, *ApJ*, 413, L101.
 Lazzati D., Ramirez-Ruiz E., Ghisellini G., 2001, *A&A*, 379, L39
 Lattimer J. M., Schramm D. N., 1976, *ApJ*, 210, 549
 Lee W. H., Ramirez-Ruiz E., 2002, *ApJ*, 577, 893
 Levinson A., Eichler D., 2000, *PhRvL*, 85, 236 (LE)
 Mészáros, P. 2002, *Annu. Rev. Astron. Astrophys.* 40, 137
 Mochkovitch R., Hernanz M., Isern J., Martin X., 1993, *Nature*, 361, 236
 Narayan R., Paczyński B., Piran T., 1992, *ApJ*, 395, L83
 Paczyński B., 1986, *ApJ*, 308, L43
 Paczyński B., 1991, *Acta Astron.*, 41, 257
 Panaiteescu A., Kumar P., Narayan R., 2001, *ApJ*, 561, L171
 Phinney E. S., 1991, *ApJ*, 380, L17
 Popham R., Woosley S. E., Fryer C., 1999, *ApJ*, 518, 356
 Qian Y. Z., Woosley S. E., 1996, *ApJ*, 471, 331
 Rosswog S., et al. 1999, *A&A*, 341, 499R
 Rosswog S., Davies M. B. 2002, *MNRAS*, 334, 481
 Rosswog S., Ramirez-Ruiz E., 2002, *MNRAS*, 336, L7
 Rosswog S., Liebendörfer M., 2003, *MNRAS* in press
 Rosswog S., Ramirez-Ruiz E., Davies M. B., 2003, *MNRAS* submitted
 Ruffert M. et al., 1997, *A&A*, 319, 122
 Ruffert M., Janka H.-T., 1999, *A&A*, 344, 573
 Schmidt M., 2001, *ApJ*, 552, 36
 Shen H., Toki H., Oyamatsu K., Sumiyoshi K., 1998a, *Nuclear Physics A*, 637, 435
 Shen H., Toki H., Oyamatsu K., Sumiyoshi, K., 1998b, *Progress of Theoretical Physics*, 100, 1013
 Thorsett S. E., Chakrabarty D., 1999, *ApJ*, 512, 288